

Effect of quartic-quintic beyond-mean-field interactions on a self-bound dipolar droplet

Luis E. Young-S.^a, S. K. Adhikari^{b,*}

^a*Grupo de Modelado Computacional, Facultad de Ciencias Exactas y Naturales, Universidad de Cartagena, 130014 Cartagena, Bolivar, Colombia*

^b*Instituto de Física Teórica, UNESP - Universidade Estadual Paulista, 01.140-070 São Paulo, São Paulo, Brazil*

Abstract

We study the effect of beyond-mean-field quantum-fluctuation (QF) Lee-Huang-Yang (LHY) and three-body interactions, with quartic and quintic nonlinearities, respectively, on the formation of a stable self-repulsive (positive scattering length a) and a self-attractive (negative a) self-bound dipolar Bose-Einstein condensate (BEC) droplet in free space under the action of two-body contact and dipolar interactions. Previous studies of dipolar droplets considered either the LHY interaction or the three-body interaction, as either of these interactions could stabilize a dipolar BEC droplet against collapse. We find that the effect of three-body recombination on the formation of a dipolar droplet could be quite large and for a complete description of the problem both the QF LHY *and* three-body interactions should be considered simultaneously, where appropriate. In the self-repulsive case for small a and in the self-attractive case, no appropriate LHY interaction is known and only three-body interaction should be used, otherwise both beyond-mean-field interactions should be used. We consider a numerical solution of a highly-nonlinear beyond-mean-field model as well as a variational approximation to it in this investigation and present results for size, shape and energy of a dipolar droplet of polarized ^{164}Dy atoms. The shape is filament-like, along the polarization direction, and could be long, for a large number of atoms N , short for small N , thin for negative a and small positive a , and fat for large positive a .

1. Introduction

An one-dimensional (1D) bright soliton remains bound due to a balance between defocusing forces and nonlinear attraction and can travel at a constant velocity [1] without deformation. Solitons have been found on water surface, in nonlinear optics [2] and in Bose-Einstein condensate (BEC) [3]. An 1D integrable analytic soliton with strict momentum and energy conservation guarantees shape preservation. In a self-attractive ($a < 0$) cigar-shaped BEC with atomic scattering length a , quasi-1D solitons have been observed [3] by applying strong confining traps in transverse directions, following a theoretical suggestion [4]. A BEC soliton with only attractive contact interaction cannot be realized [5] in two (2D) and three (3D) dimensions due to a collapse instability.

Nevertheless, there has been intense research activity on a self-bound BEC in free space. In 2D and 3D, a self-bound spinor BEC can be formed in the presence of a spin-orbit coupling interaction [6]. The spin-orbit coupling can generate an effective interatomic repulsion at short distances cancelling the mean-field attraction and stabilize the spinor BEC against collapse [7]. In 3D, the inclusion of a quantum-fluctuation (QF) Lee-Huang-Yang (LHY) interaction [8] or of repulsive three-body interaction [9], in the beyond-mean-field model of a BEC, can stop the collapse and thus produce a self-bound BEC [10], self-bound binary BEC [11] and a self-bound binary Bose-Fermi superfluid mixture [12]. The LHY interaction in the binary mixture arises due to the QF correction appropriate to the repulsive intraspecies interaction [11]. Self-bound binary BECs of ^{39}K atoms have been observed [13]. The role of

*Corresponding author.

Email addresses: lyoung@unicartagena.edu.co (Luis E. Young-S.), sk.adhikari@unesp.br (S. K. Adhikari)

URL: professores.ift.unesp.br/sk.adhikari/ (S. K. Adhikari)

the three-body interaction in atomic systems have been emphasized from an experimental [14] point of view as well as in self-bound condensates [10], harmonically-trapped condensates [15] and in condensates on optical lattices [16].

In a different front, high-density droplets were observed in a trapped strongly dipolar BEC of ^{164}Dy [17, 18] and ^{168}Er [19] atoms. In the framework of a beyond-mean-field model, the QF LHY interaction, appropriately modified for dipolar atoms, [20] can stabilize [21] such a strongly dipolar BEC droplet against collapse. A self-bound dipolar BEC can also be formed in free space under the action of the QF LHY interaction in the self-repulsive case ($a > 0$) [22, 23, 24] or under the action of the three-body interaction [25]. Higher-order nonlinearities can also stabilize a self-attractive nondipolar BEC and form a self-bound droplet in 3D [26]. A 3D self-bound BEC, although bears some similarity with a soliton, does not satisfy the strict energy and momentum conservation laws of an analytic 1D soliton and is called a droplet.

In this paper we study the formation of a self-bound self-repulsive and self-attractive dipolar droplet of ^{164}Dy atoms, polarized along the z direction, including both the QF LHY and three-body interactions. Presently, the QF LHY interaction for dipolar atoms, appropriate for the calculation of stationary states, is “known” [20] only in the self-repulsive case for dipolar length a_{dd} , viz. (2), satisfying $a_{\text{dd}} < a$, where this interaction is real, or for $a_{\text{dd}} \gtrsim a$, where this interaction is complex with a negligible imaginary part. In the domain $a_{\text{dd}} < a$ the system is too repulsive and no self-bound droplet can be formed. For $a_{\text{dd}} \gg a$, the imaginary part becomes large and the present form of LHY interaction [20] should not be used for the calculation of stationary droplet states [27]. Nevertheless, for $a_{\text{dd}} \gg a$, a real three-body interaction alone can lead to a self-bound dipolar droplet and will be employed in this study. We find that the three-body interaction may have a substantial effect on the formation of a droplet, specially, on its energy, shape and size, for small a . The dipolar droplets have a filament-like shape, along z direction, which can be long for large N and short for small N , fat for large positive a , and thin for negative a and small positive a . In previous studies [21, 22, 23] only long filament-like droplets for large N were found and highlighted in the self-repulsive case stabilized by the QF LHY interaction alone. The QF LHY and three-body interactions are the two beyond-mean-field interaction of lowest and next-to-lowest orders, with quartic and quintic nonlinearities, respectively, and for a complete description of the formation of a self-bound dipolar droplet, we will consider both these interactions, where appropriate, in both self-repulsive and self-attractive cases. For large a ($a_{\text{dd}}/4 \lesssim a < a_{\text{dd}}$) we consider both QF LHY and three-body interactions and for small a ($a \lesssim a_{\text{dd}}/4$) only the three-body interaction is considered. We consider a numerical solution of the underlying beyond-mean-field model including the QF LHY interaction and a repulsive three-body interaction. For an analytic understanding of the results we also employ a variational approximation to the beyond-mean-field model.

In Sec. 2 we present the beyond-mean-field model including the QF LHY and three-body interactions as well as an analytic variational approximation to this model using a Gaussian ansatz for the wave function. The use of this ansatz leads to an analytic approximation to energy and a minimization of this energy with respect to the widths of the wave function fixes the energy as well as the widths of the self-bound droplet. In Sec. 3 we present the variational results for energy and root-mean-square (rms) size of 3D self-bound BEC droplets of ^{164}Dy atoms and compare these with the same obtained from a numerical solution of the beyond-mean-field model. Finally, in Sec. 4 we present a summary of our findings.

2. Beyond-Mean-field model

In this paper we base our study on a 3D beyond-mean-field model, including the quantum-fluctuation LHY interaction and three-body repulsion, for a self-bound dipolar droplet. We consider a BEC of N dipolar ^{164}Dy atoms polarized along the z axis, of mass m each, interacting through the following atomic dipolar and contact interactions [28, 29, 30]

$$V(\mathbf{R}) = \frac{\mu_0 \mu^2}{4\pi} \frac{1 - 3 \cos^2 \theta}{|\mathbf{R}|^3} + \frac{4\pi \hbar^2 a}{m} \delta(\mathbf{R}), \quad (1)$$

where μ_0 is the permeability of vacuum, μ is the magnetic dipole moment of an atom, $\mathbf{R} = \mathbf{r} - \mathbf{r}'$ is the vector joining two dipoles placed at $\mathbf{r} \equiv \{x, y, z\}$ and $\mathbf{r}' \equiv \{x', y', z'\}$ and θ is the angle made by \mathbf{R} with the z axis. To compare the dipolar interaction with the contact interaction, it is convenient to express the strength of dipolar interaction $\mu_0 \mu^2 / 4\pi$

in terms of the dipolar length:

$$a_{\text{dd}} \equiv \frac{\mu_0 \mu^2 m}{12\pi \hbar^2}. \quad (2)$$

The dimensionless ratio

$$\varepsilon_{\text{dd}} \equiv \frac{a_{\text{dd}}}{a} \quad (3)$$

then determines the relative strength of dipolar interaction compared to contact interaction and controls many properties of a dipolar BEC. For the formation of a self-bound dipolar droplet, the dipolar length a_{dd} should necessarily be greater than the scattering length: $a_{\text{dd}} > a$, thus requiring a strongly dipolar atom, where the dipolar interaction dominates over the contact interaction to make the system attractive. Hence in this study we employ ^{164}Dy atoms with large dipole moment $\mu = 10\mu_{\text{B}}$, where μ_{B} is the Bohr magneton. The dipolar length of ^{164}Dy atoms is $a_{\text{dd}} = 130.8a_0$ and is larger than its experimental scattering length $a = (92 \pm 8)a_0$ [31], where a_0 is the Bohr radius. Consequently, a BEC of ^{164}Dy atoms can naturally host a droplet in free space without any tuning of the scattering length to an appropriate value using a Feshbach resonance as usually required in engineering a soliton in nondipolar atoms [3, 13]. However, in this study we will consider the whole domain $a_{\text{dd}} > a$ where a droplet can be formed.

A *trapless* dipolar BEC droplet is described by the following 3D beyond-mean-field Gross-Pitaevskii (GP) equation [28, 29, 32] including the QF LHY interaction [30, 33] and a repulsive three-body interaction

$$i\hbar \frac{\partial \psi(\mathbf{r}, t)}{\partial t} = \left[-\frac{\hbar^2}{2m} \nabla^2 + \frac{4\pi \hbar^2}{m} a N |\psi(\mathbf{r}, t)|^2 + \frac{3\hbar^2}{m} a_{\text{dd}} N \int \frac{1 - 3 \cos^2 \theta}{|\mathbf{R}|^3} |\psi(\mathbf{r}', t)|^2 d\mathbf{r}' \right. \\ \left. + \frac{\gamma_{\text{QF}} \hbar^2}{m} N^{\frac{3}{2}} |\psi(\mathbf{r}, t)|^3 + \frac{\hbar N^2 K_3}{2} |\psi(\mathbf{r}, t)|^4 \right] \psi(\mathbf{r}, t), \quad (4)$$

where K_3 is the strength of the three-body interaction with quintic nonlinearity and γ_{QF} is the strength of the QF LHY interaction with quartic nonlinearity, and the wave function is normalized as $\int |\psi(\mathbf{r}, t)|^2 d\mathbf{r} = 1$. The three-body coefficient K_3 is small and actually complex. The imaginary part of this term, not considered here, and usually considered in other studies [34], is responsible for a loss of atoms from the condensate due to molecule formation by three-body recombination. The importance of the real part of this term has been emphasized in different investigations and used in the study of harmonically-trapped condensates [15], self-bound 3D droplets [10] and condensates on optical lattices [16]. In this study we will ignore the imaginary part of K_3 and take K_3 to be real and *positive* (repulsive) as we will be concerned here with a stationary state and not a decaying nonstationary state, where an imaginary K_3 is appropriate. The real K_3 , considered here, with a higher-order quintic nonlinearity, can stabilize [10] a self-bound dipolar droplet against collapse in free space.

The coefficient of the beyond-mean-field LHY-type quantum correction term γ_{QF} is given by [20, 33]

$$\gamma_{\text{QF}} = \frac{128}{3} \sqrt{\pi a^5} Q_5(\varepsilon_{\text{dd}}), \quad (5)$$

where the auxiliary function

$$Q_5(\varepsilon_{\text{dd}}) = \int_0^1 dx (1 - x + 3x\varepsilon_{\text{dd}})^{\frac{5}{2}}. \quad (6)$$

can be evaluated to yield an analytic expression for the QF coefficient [33]

$$\gamma_{\text{QF}} = \frac{128}{3} \sqrt{\pi a^5} \frac{(3\varepsilon_{\text{dd}})^{\frac{5}{2}}}{48} \left[(8 + 26\varepsilon + 33\varepsilon^2) \sqrt{1 + \varepsilon} - 15\varepsilon^3 \ln \left(\frac{1 + \sqrt{1 + \varepsilon}}{\sqrt{\varepsilon}} \right) \right], \quad \varepsilon = \frac{1 - \varepsilon_{\text{dd}}}{3\varepsilon_{\text{dd}}}, \quad (7)$$

$$\approx \frac{128}{3} \sqrt{\pi a^5} \left(1 + \frac{3}{2} \varepsilon_{\text{dd}}^2 \right). \quad (8)$$

Actually, the function Q_5 as well as the coefficient γ_{QF} , representing a correction for dipolar atoms, is complex for $\varepsilon_{\text{dd}} > 1$ and, for studies of stationary states, expression (7) is formally meaningful for $\varepsilon_{\text{dd}} \leq 1$, where this expression is real [27]. However its imaginary part remains small compared to its real part for medium values of a where

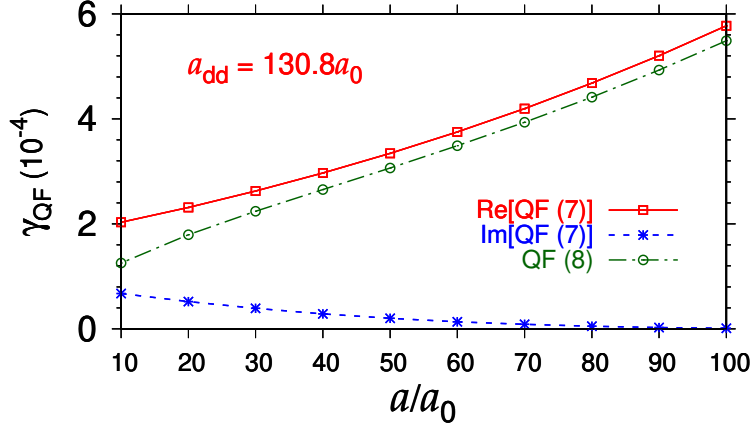


Figure 1: Real (Re) and imaginary (Im) parts of the exact LHY QF coefficient (7) and its real approximation (8) versus scattering length a for dipolar ^{164}Dy atoms. Plotted quantities are dimensionless and the physical unit for ^{164}Dy atoms can be restored using the unit of length $l = 1 \mu\text{m}$.

$4 \gtrsim \varepsilon_{\text{dd}} > 1$ and will be neglected in this study of stationary self-bound states as in other studies, consistent with the neglect of the imaginary part of the three-body coefficient K_3 . For nondipolar atoms $\varepsilon_{\text{dd}} = 0$, while $Q_5(\varepsilon_{\text{dd}}) = 1$, and one recovers the well-known LHY limit $\gamma_{\text{QF}} = 128 \sqrt{\pi a^5}/3$ [8] valid for repulsive hard-sphere nondipolar atoms. The approximation (8) to QF coefficient, advocated in Ref. [33] for small ε_{dd} , has often been used in different studies [22, 23, 35, 36] for $\varepsilon_{\text{dd}} > 1$. In Fig. 1 we display the real and imaginary parts of the QF coefficient (7) and its real approximation (8) for different values of a . From Fig. 1, we find that the agreement between the two forms QF coefficients is satisfactory for larger values of a ($a \gtrsim 30a_0$), where the QF LHY interaction has a small imaginary part. In this domain, the QF LHY interaction will be used in conjunction with the three-body interaction in the study of stationary dipolar self-bound droplets. For smaller values of a ($a \lesssim 30a_0$), where the imaginary part of the LHY interaction is large and in the self-attractive case, where the QF interaction is not known, we will use only the three-body interaction in the study of the self-bound dipolar droplets.

Equation (4) can be reduced to the following dimensionless form by scaling lengths in units of a fixed length scale $l = 1 \mu\text{m}$, time in units of ml^2/\hbar , density $|\psi|^2$ in units of l^{-3} , K_3 in units of $\hbar l^4/m$, and energy in units of \hbar^2/ml^2

$$i \frac{\partial \psi(\mathbf{r}, t)}{\partial t} = \left[-\frac{1}{2} \nabla^2 + 3a_{\text{dd}} N \int \frac{1 - 3 \cos^2 \theta}{|\mathbf{R}|^3} |\psi(\mathbf{r}', t)|^2 d\mathbf{r}' + 4\pi a N |\psi(\mathbf{r}, t)|^2 + \gamma_{\text{QF}} N^{\frac{3}{2}} |\psi(\mathbf{r}, t)|^3 + \frac{K_3 N^2}{2} |\psi(\mathbf{r}, t)|^4 \right] \psi(\mathbf{r}, t). \quad (9)$$

Equation (9) can also be obtained by applying the variational rule

$$i \frac{\partial \psi}{\partial t} = \frac{\delta E}{\delta \psi^*} \quad (10)$$

with the following energy functional (energy per atom) of a stationary dipolar droplet

$$E = \int d\mathbf{r} \left[\frac{|\nabla \psi(\mathbf{r})|^2}{2} + 2\pi N a |\psi(\mathbf{r})|^4 + \frac{3}{2} a_{\text{dd}} N |\psi(\mathbf{r})|^2 \int \frac{1 - 3 \cos^2 \theta}{R^3} |\psi(\mathbf{r}')|^2 d\mathbf{r}' + \frac{2\gamma_{\text{QF}}}{5} N^{\frac{3}{2}} |\psi(\mathbf{r})|^5 + \frac{K_3 N^2}{6} |\psi(\mathbf{r})|^6 \right]. \quad (11)$$

For a self-bound droplet this energy has to be negative necessarily.

The formation of a self-bound dipolar droplet can be understood by an analytic variational approximation obtained

with the following normalized axisymmetric Gaussian ansatz for the stationary wave function:

$$\psi(\mathbf{r}) = \frac{\pi^{-\frac{3}{4}}}{\sqrt{w_z w_\rho}} \exp\left[-\frac{\rho^2}{2w_\rho^2} - \frac{z^2}{2w_z^2}\right], \quad (12)$$

where $\rho \equiv \{x, y\}$, w_z and w_ρ are the widths of the Gaussian wave function. With this function, the energy integral (11) can be evaluated to yield the following analytical result [29]

$$E = \frac{1}{2w_\rho^2} + \frac{1}{4w_z^2} + \frac{N[a - a_{\text{dd}}f(\kappa)]}{\sqrt{2\pi}w_\rho^2 w_z} + \left(\frac{2}{5}\right)^{\frac{5}{2}} \frac{\gamma_{\text{QF}} N^{\frac{3}{2}}}{\pi^{\frac{9}{4}} w_\rho^3 w_z^{\frac{3}{2}}} + \frac{K_3 N^2 \pi^{-3}}{18 \sqrt{3} w_\rho^4 w_z^2}, \quad \kappa = \frac{w_\rho}{w_z}, \quad (13)$$

where

$$f(\kappa) = \frac{1 + 2\kappa^2 - 3\kappa^2 d(\kappa)}{1 - \kappa^2}, \quad (14)$$

$$d(\kappa) = \frac{\text{atanh} \sqrt{1 - \kappa^2}}{\sqrt{1 - \kappa^2}}. \quad (15)$$

In Eq. (13), the first two terms on the right hand side are contributions of the kinetic energy of an atom in the droplet, the third term on the right hand side corresponds to the net attractive atomic interactions responsible for the formation of a self-bound droplet and the last two terms are contributions of the beyond-mean-field QF LHY and repulsive three-body interactions, respectively. The higher order quartic and quintic nonlinearities of the QF LHY and three-body interactions compared to the cubic nonlinearity of the two-body interaction, has led to a more singular repulsive term at the center ($w_\rho, w_z \rightarrow 0$) in (13). This makes the system highly repulsive at the center and stops the collapse stabilizing the self-bound dipolar droplet.

A minimization of energy (13) with respect to widths w_ρ ($\partial E/\partial w_\rho = 0$) and w_z ($\partial E/\partial w_z = 0$) determines the widths of the self-bound dipolar BEC

$$\frac{1}{w_\rho^3} + \frac{N[2a - a_{\text{dd}}g(\kappa)]}{\sqrt{2\pi}w_\rho^3 w_z} + \left(\frac{2}{5}\right)^{\frac{5}{2}} \frac{3\gamma_{\text{QF}} N^{\frac{3}{2}}}{\pi^{\frac{9}{4}} w_\rho^4 w_z^{\frac{3}{2}}} + \frac{4K_3 N^2}{18 \sqrt{3} \pi^3 w_\rho^5 w_z^2} = 0, \quad (16)$$

$$\frac{1}{w_z^3} + \frac{2N[a - a_{\text{dd}}c(\kappa)]}{\sqrt{2\pi}w_\rho^2 w_z^2} + \left(\frac{2}{5}\right)^{\frac{5}{2}} \frac{3\gamma_{\text{QF}} N^{\frac{3}{2}}}{\pi^{\frac{9}{4}} w_\rho^3 w_z^{\frac{5}{2}}} + \frac{4K_3 N^2}{18 \sqrt{3} \pi^3 w_\rho^4 w_z^3} = 0, \quad (17)$$

where

$$g(\kappa) = \frac{2 - 7\kappa^2 - 4\kappa^4 + 9\kappa^4 d(\kappa)}{(1 - \kappa^2)^2}, \quad (18)$$

$$c(\kappa) = \frac{1 + 10\kappa^2 - 2\kappa^4 - 9\kappa^2 d(\kappa)}{(1 - \kappa^2)^2}. \quad (19)$$

The widths, obtained from a solution of Eqs. (16) and (17), when substituted in Eq. (13), determine the corresponding energy.

3. Numerical Results

We solve 3D partial differential equation (9) for a dipolar BEC numerically by the split-time-step Crank-Nicolson method [37] employing the imaginary-time propagation rule. There are FORTRAN/C programs [29] and their open-multiprocessing versions [38] appropriate for this purpose. Often, the self-bound dipolar droplet is highly elongated along the z direction; in such cases it is appropriate to take a larger number of discretization points along the z direction as compared to x and y directions. It is difficult to treat numerically the dipolar interaction integral in Eq. (9) in configuration space due to the problematic $1/|\mathbf{R}|^3$ term. The dipolar interaction integral is evaluated in the

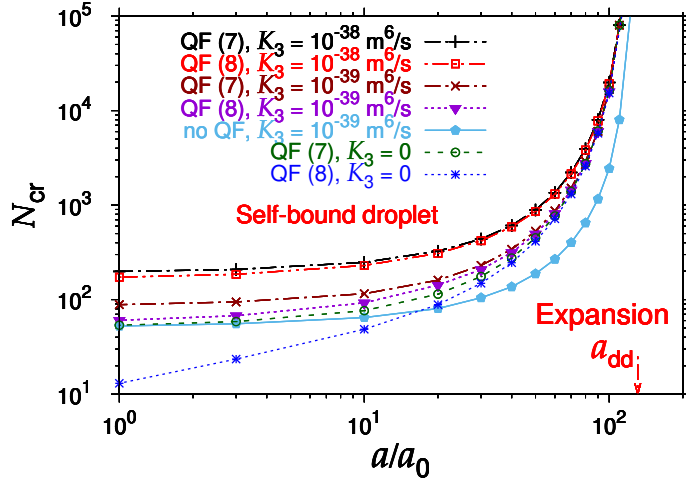


Figure 2: Variational critical number of atoms N_{cr} for the formation of a self-bound dipolar droplet for $K_3 = 0$, $K_3 = 10^{-39} \text{ m}^6/\text{s}$, and $K_3 = 10^{-38} \text{ m}^6/\text{s}$ and QF coefficients (7) and (8). A result with zero QF coefficient (no QF) is also shown. For $N > N_{\text{cr}}$ a self-bound dipolar droplet can be formed. For $a > a_{\text{dd}}$ and for $N < N_{\text{cr}}$ there is expansion to infinity and no droplet can be formed. Plotted quantities are dimensionless.

momentum space by a Fourier transformation and this is advantageous numerically as that integral in momentum space has a smooth behavior. The Fourier transformation of the dipolar potential can also be obtained analytically and this aids in the numerical solution of Eq. (9) [29]. After evaluation in momentum space, the results are transformed back to configuration space by a backward Fourier transformation.

In numerical calculation, we use the parameters of ^{164}Dy atoms, e.g., $a_{\text{dd}} = 130.8a_0$ and $m = 164 \text{ amu}$. The parameter K_3 is not experimentally known but it should have a small effect, compared to the usual two-body term, proportional to $4\pi a$, in Eq. (9). The order of magnitude of the imaginary part of K_3 is known [34] and we take the real part of K_3 in this study to have similar values. Here we consider $K_3 = 10^{-39} \text{ m}^6/\text{s}$ and $K_3 = 10^{-38} \text{ m}^6/\text{s}$. With the unit of length $l = 1 \mu\text{m}$, we have for unit of time $m l^2 / \hbar = 2.58 \text{ ms}$, for unit of 3D density $l^{-3} = 1 \mu\text{m}^{-3}$, for unit of energy $\hbar^2 / (m l^2) = 4.08 \times 10^{-32} \text{ J}$, and for unit of K_3 $\hbar l^4 / m = 3.87 \times 10^{-34} \text{ m}^6/\text{s}$. To study the effect of a variation of the scattering length a on the formation of a self-bound dipolar BEC, we vary the scattering length for values smaller than its experimental value $a = (92 \pm 8)a_0$ [31]. In an experiment, a variation of the value of scattering length is effected by manipulating an external magnetic field near a Feshbach resonance [39]. For the formation of a dipolar droplet, we need a strongly dipolar BEC with $\varepsilon_{\text{dd}} > 1$ and a BEC of ^{164}Dy atoms with experimental $\varepsilon_{\text{dd}} \equiv a_{\text{dd}}/a = 1.4217 > 1$ is an ideal candidate for the same.

The effect of different beyond-mean-field interactions – the QF LHY interaction (7), its approximation (8), and the three-body interaction – on the formation of a dipolar droplet in free space for different a and N can be qualitatively understood from a consideration of the analytic variational energy (13). In Eq. (13), all terms are positive (repulsive) except the contact and dipolar interaction terms involving a and a_{dd} , respectively. For the formation of a self-bound droplet, the energy (13) has to be negative for certain w_ρ and w_z , and that happens for N larger than a critical value N_{cr} , while Eqs. (16) and (17), for variational widths w_ρ and w_z , allow real solutions. For $N < N_{\text{cr}}$ the system is much too repulsive and undergoes an expansion to infinity without the formation of a droplet. However, the critical number N_{cr} is a function of the three-body coefficient K_3 and scattering length a . The scattering length a can be controlled experimentally, independent of the three-body coefficient K_3 , by using an optical [40] or a magnetic [39] Feshbach resonance. There are also different suggestions for controlling K_3 similarly [41]. As a increases, the system becomes less attractive and it is possible to have a negative energy only for a larger N . Consequently, N_{cr} increases as a increases for a fixed K_3 . Similarly, a non-zero K_3 makes the system less attractive and a larger N is needed to make the energy negative. Hence N_{cr} should increase monotonically with K_3 , while a is held fixed. The $N_{\text{cr}}-a$ correlation for $K_3 = 0$, $= 10^{-39} \text{ m}^6/\text{s}$, and $= 10^{-38} \text{ m}^6/\text{s}$, is shown in Fig. 2 for QF LHY interaction (7) and its often used [22, 23, 33, 35, 36] approximation (8). To demonstrate that the three-body repulsion alone can form a self-bound droplet, we also display in Fig. 2 the result for $K_3 = 10^{-39} \text{ m}^6/\text{s}$ with no LHY interaction. For small K_3 ($K_3 = 0$ and

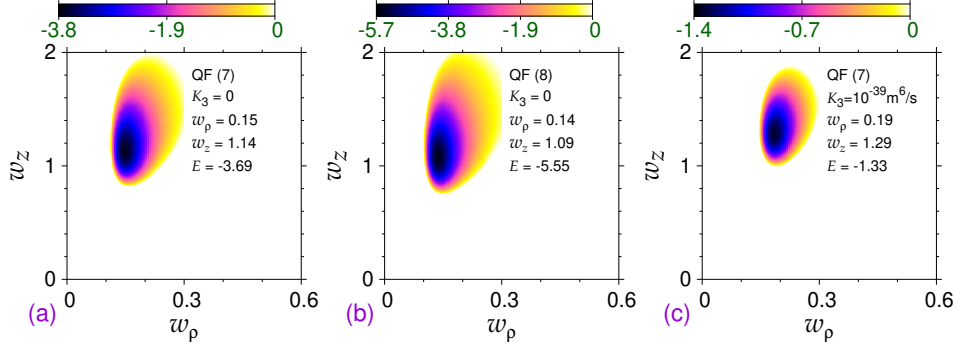


Figure 3: 2D contour plot of variational energy per atom (13) highlighting its minimum value and the negative energy region for $a = 60a_0$, $N = 1000$ ^{164}Dy atoms, as a function of widths w_ρ and w_z for (a) $K_3 = 0$, QF coefficient (7), (b) $K_3 = 0$, QF coefficient (8), and (c) $K_3 = 10^{-39} \text{ m}^6/\text{s}$, QF coefficient (7). Plotted quantities are dimensionless and the physical unit for ^{164}Dy atoms can be restored using the unit of length $l = 1 \mu\text{m}$.

$K_3 = 10^{-39} \text{ m}^6/\text{s}$) and small a , the $N_{\text{cr}}-a$ correlation of Fig. 2 is sensitive to the form of QF coefficient – Eq. (7) or Eq. (8). For a large K_3 ($K_3 = 10^{-38} \text{ m}^6/\text{s}$), the associated strong three-body repulsion dominates at short distances, that musks the effect of QF LHY interaction, and the result is not sensitive to the form of γ_{QF} . The result with zero QF LHY interaction and $K_3 = 10^{-39} \text{ m}^6/\text{s}$ is quite similar to the result with QF LHY interaction (7) and $K_3 = 0$, specially for small a ; in that case the use of K_3 alone is recommended for the study of dipolar droplets.

In Fig. 3 we display the 2D contour plot of variational energy (13) as a function of widths w_ρ and w_z for different beyond-mean-field interactions and $N = 1000$, $a = 60a_0$. The plots in this figure highlight the negative energy region for different w_ρ and w_z . The minimum negative energy in these plots corresponds to a self-bound dipolar droplet. The white region in these plots corresponds to positive energy. If we compare plots 3(a) and (b) we find that an increased attraction due to the use of approximate QF coefficient has reduced the energy by about 50%. Similarly, comparing plots 3(a) and (c), we find that the inclusion of a moderately repulsive three-body interaction has increased the energy by about 60%. In both cases there has been a change in the profile of the self-bound state with a change in the widths w_ρ and w_z due to the use of different beyond-mean-field interactions (result not presented in this paper).

To demonstrate that the formation of a self-bound droplet remains sensitive to the use of different beyond-mean-

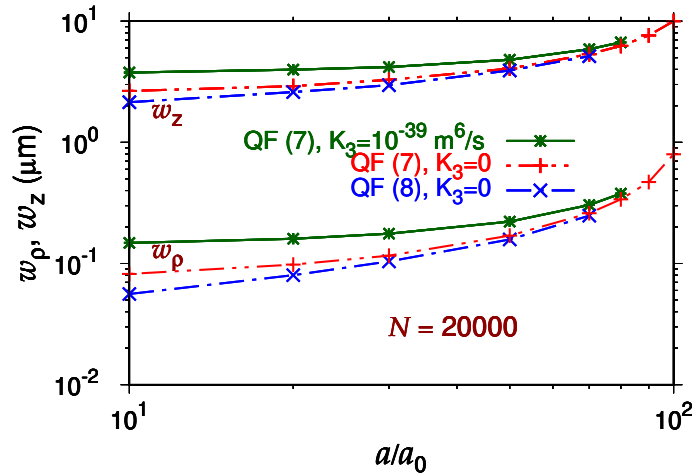


Figure 4: Variational results for widths w_ρ and w_z for different beyond-mean-field interaction. The lines are labeled by the QF coefficients (7) and (8) and the values of the three-body coefficient K_3 .

Table 1: Variation and numerical energy E , rms size $\langle x \rangle \equiv w_\rho / \sqrt{2}$ and $\langle z \rangle \equiv w_z / \sqrt{2}$ of self-bound axially-symmetric dipolar droplets of ^{164}Dy atoms in dimensionless units for different a , N , γ_{QF} and K_3 .

a (a_0)	N (10^3)	γ_{QF}	K_3 (m^6/s)	Variational			Numerical		
				$\langle x \rangle$	$\langle z \rangle$	E	$\langle x \rangle$	$\langle z \rangle$	E
90	10	(7)	0	0.32	4.02	-0.74	0.34	3.83	-0.95
90	10	(7)	10^{-39}	0.35	4.20	-0.59	0.36	4.01	-0.76
90	10	(7)	10^{-38}	0.50	5.22	-0.14	0.53	5.00	-0.23
90	10	(8)	0	0.31	3.89	-0.93	0.32	3.70	-1.15
90	10	(8)	10^{-39}	0.33	4.09	-0.72	0.35	3.89	-0.92
90	10	(8)	10^{-38}	0.49	5.12	-0.17	0.51	4.77	-0.26
30	0.3	(7)	0	0.042	0.29	-46.3	0.045	0.27	-56.2
30	0.3	(7)	10^{-39}	0.065	0.37	-10.0	0.070	0.35	-13.8
30	0.3	none	10^{-39}	0.038	0.27	-130	0.038	0.25	-141
30	0.3	(8)	0	0.037	0.26	-53.9	0.037	0.27	-69.1
30	0.3	(8)	10^{-39}	0.061	0.35	-16.2	0.063	0.33	-21.6

field interaction for a large number of atoms N , specially for small scattering lengths a , we illustrate in Fig. 4 the variational widths w_ρ and w_z of a self-bound droplet of $N = 20000$ atoms versus a for different beyond-mean-field interaction controlled by the QF coefficients (7) and (8), and three-body coefficient K_3 . We find that the widths can have a large variation for the use of different beyond-mean-field interaction for small values of a . In Fig. 1, we find that the QF coefficient (7) is more repulsive than its approximation (8). Consequently, for $K_3 = 0$, in Fig. 4 the widths obtained with the use of QF coefficient (7) are larger than the same obtained with the use of Eq. (8). The inclusion of a non-zero three-body coefficient K_3 increases the repulsion and consequently, the widths increase. Hence from Figs. 3 and 4 we find that the formation of a self-bound droplet – its shape and size – is sensitive to the use of different beyond-mean-field interaction.

In Table I we compare the variational and numerical results for the rms sizes $\langle x \rangle$, and $\langle z \rangle$ and energy per atom E of a self-bound dipolar droplet for different a , N , γ_{QF} , and K_3 . The agreement between the variational and numerical results is satisfactory. The dipolar system is more attractive for $a = 30a_0$ than for $a = 90a_0$ due to an increased contact repulsion in the latter, thus resulting in strongly-bound droplets for $a = 30a_0$ with smaller size $\langle z \rangle$ and smaller energy. The attraction also increases with a reduction in K_3 or with the use of the approximation (8) in place of the exact QF coefficient (7), leading to smaller energies and sizes.

To study the density distribution of a self-bound droplet, we calculate the reduced 1D densities

$$\rho_{1D}(x) \equiv \int dz dy |\psi(\mathbf{r})|^2, \quad (20)$$

$$\rho_{1D}(z) \equiv \int dx dy |\psi(\mathbf{r})|^2. \quad (21)$$

In Fig. 5, we plot these densities as obtained from the variational approximation and numerical calculation for $a = 30a_0$, $N = 300$, and for different beyond-mean-field interaction, e.g., (a) $K_3 = 0$ and QF coefficient (7), (b) $K_3 = 10^{-39} \text{ m}^6/\text{s}$ and QF coefficient (7), (c) $K_3 = 0$ and QF coefficient (8), and (d) $K_3 = 10^{-39} \text{ m}^6/\text{s}$ and no QF LHY interaction. The corresponding rms sizes $\langle x \rangle$ and $\langle z \rangle$ and the energy E of these self-bound droplets are presented in Table I. The increase of three-body repulsion for a fixed a and N , from Fig. 5(a) to Fig. 5(b), due to an increase in K_3 from 0 to $10^{-39} \text{ m}^6/\text{s}$, results in larger rms sizes of the self-bound dipolar droplet, viz. Table I. Similarly, the use of less repulsive QF coefficient (8) in Fig. 5(c), compared to the use of coefficient (7) in Fig. 5(a), has led to more attraction in the former with smaller sizes and smaller energy. The density profiles of Figs. 5(a) and (d) are quite similar, which suggests that it will be reasonable to replace the QF LHY interaction by a small three-body interaction for $a \lesssim 30a_0$ (both self-repulsive and self-attractive cases), as we will do in this paper.

In Fig. 6 we present 1D densities $\rho_{1D}(x)$ and $\rho_{1D}(z)$ for larger values of scattering lengths ($a = 60a_0, 90a_0$) as well as negative values of scattering lengths. Although, for $a = 30a_0$, the density profiles show a sensitivity to the inclusion of a three-body interaction with an increase of length along z direction, viz. Figs. 5(a)-(b), this sensitivity

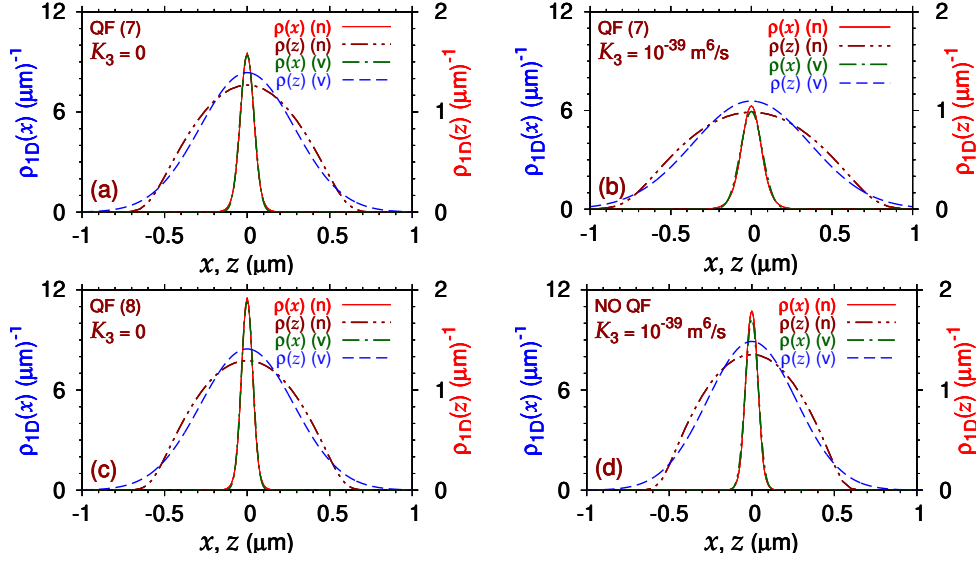


Figure 5: Numerical (n) and variational (v) reduced 1D densities $\rho_{1D}(x)$ and $\rho_{1D}(z)$ along x and z directions, respectively, of a ^{164}Dy droplet with $a = 30a_0$, $N = 300$, and (a) $K_3 = 0$, QF coefficient (7), (b) $K_3 = 10^{-39} \text{ m}^6/\text{s}$, QF coefficient (7), (c) $K_3 = 0$, QF coefficient (8), and (d) $K_3 = 10^{-39} \text{ m}^6/\text{s}$, zero QF coefficient.

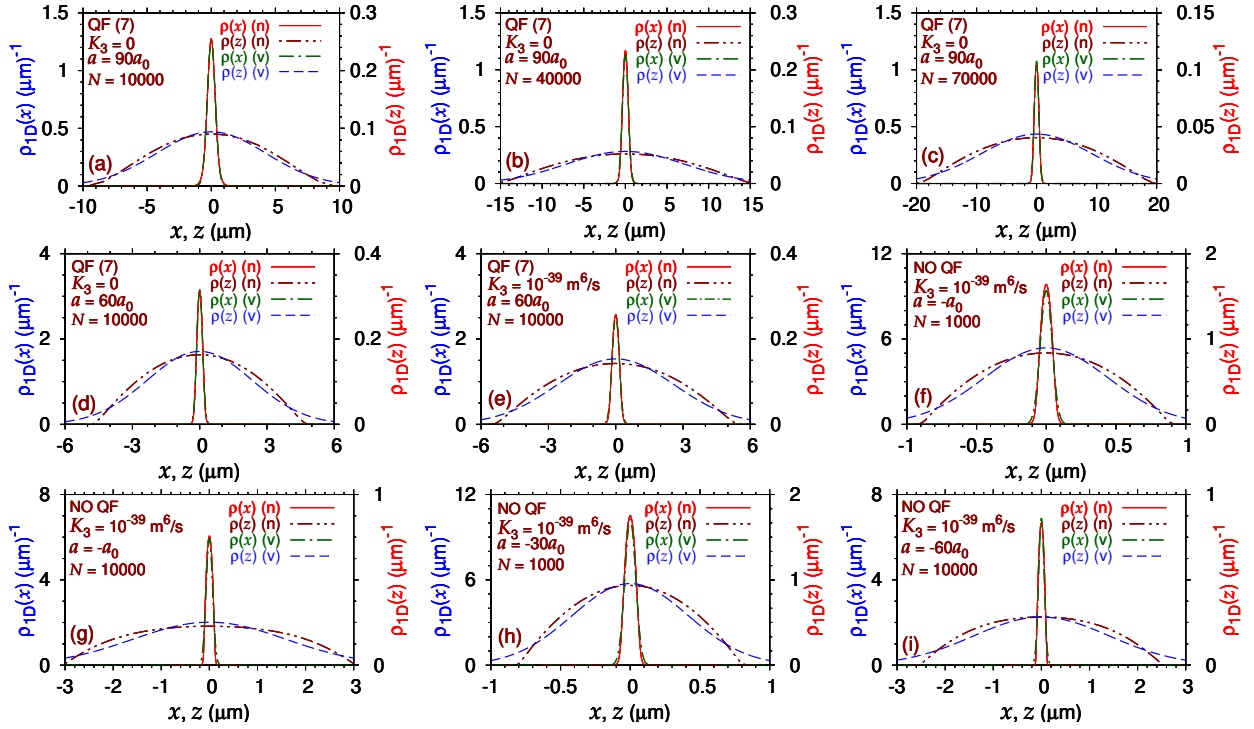


Figure 6: Numerical (n) and variational (v) reduced 1D densities $\rho_{1D}(x)$ and $\rho_{1D}(z)$ along x and z directions, respectively, of a ^{164}Dy droplet with (a) $a = 90a_0$, $N = 10000$, (b) $a = 90a_0$, $N = 40000$, (c) $a = 90a_0$, $N = 70000$, (d) $a = 60a_0$, $N = 10000$, (e) $a = 60a_0$, $N = 10000$, (f) $a = -a_0$, $N = 1000$, (g) $a = -a_0$, $N = 10000$, (h) $a = -30a_0$, $N = 1000$, and (i) $a = -60a_0$, $N = 10000$. In (a)-(e) QF coefficient (7) is used and in (f)-(i) there is no QF correction. In (a)-(d) $K_3 = 0$ and $K_3 = 10^{-39} \text{ m}^6/\text{s}$ in others.

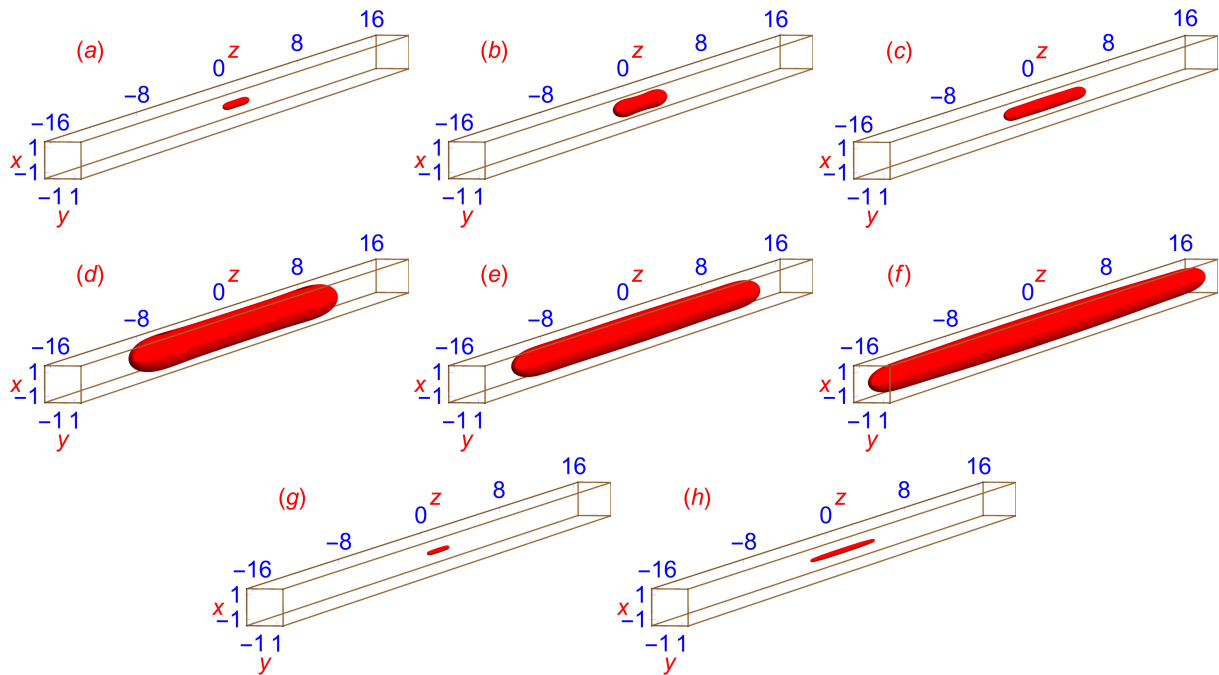


Figure 7: Isodensity contour of 3D density $|\psi(x, y, z)|^2$ for (a) $a = 30a_0, N = 300$, (b) $a = 60a_0, N = 1000$, (c) $a = 60a_0, N = 10000$, (d) $a = 90a_0, N = 10000$, (e) $a = 90a_0, N = 20000$, (f) $a = 90a_0, N = 40000$, (g) $a = -a_0, N = 1000$, (h) $a = -60a_0, N = 10000$. In (a)-(f) $K_3 = 0$ and QF coefficient (7) is employed, and in (g)-(h) $K_3 = 10^{-39} \text{ m}^6/\text{s}$, and no QF correction is used. The density $|\psi(x, y, z)|^2$ on the contour is 10^{-8} cm^{-3} and the units of x, y, z are μm .

is much reduced for larger a , as illustrated in Figs. 6(d)-(e) for $a = 60a_0$ and $N = 10000$, where the z -length is practically unchanged after the inclusion of the three-body interaction. For $a = 90a_0$, the sensitivity to the inclusion of a three-body interaction is further reduced (not illustrated in this paper) and in Figs. 6(a)-(c) we display the linear densities for $a = 90a_0, K_3 = 0$ and QF LHY interaction (7) for $N = 10000, 40000$ and 70000 , respectively. The z -length gradually increases as N is increased from 10000 to 40000 to 70000 in Figs. 6(a)-(c) due to an increase of contact repulsion for an increased number of atoms. In the self-repulsive case, the z -length also increases, due to an increased repulsion, with an increased a for a fixed $N (=10000)$, viz. Figs. 6(a) and (d). For smaller a ($a \lesssim 30a_0$), the imaginary part of the QF LHY interaction is large and the use of this interaction is not recommended [27]. However, it seems highly unlikely that a self-bound dipolar droplet will cease to exist in this domain and in that case, we employ only the three-body interaction in the study of the formation of a dipolar droplet. In Fig. 6, we further display the linear densities for $K_3 = 10^{-39} \text{ m}^6/\text{s}$, and (f) $a = -a_0, N = 1000$, (g) $a = -a_0, N = 10000$, (h) $a = -30a_0, N = 1000$, and (i) $a = -60a_0, N = 10000$, where no QF LHY interaction is included. In the self-attractive case, the z -length slightly decreases with an increased $|a|$ for a fixed N due to an increased attraction as can be found from Figs. 6(f) and (h), and 6(g) and (i); similarly, the z -length increases with an increased N for a fixed $a (= -a_0)$ as can be found from Figs. 6(f) and (g).

The change in size and shape of a self-bound dipolar droplet with an increase of number of atoms N or of scattering length a is best illustrated by an isodensity plot of the 3D profile. In Fig. 7 we display the isodensity contour of 3D density $|\psi(x, y, z)|^2$ of a self-bound dipolar droplet for (a) $a = 30a_0, N = 300$, (b) $a = 60a_0, N = 1000$, (c) $a = 60a_0, N = 10000$, (d) $a = 90a_0, N = 10000$, (e) $a = 90a_0, N = 20000$, (f) $a = 90a_0, N = 40000$, (g) $a = -a_0, N = 1000$, (h) $a = -60a_0, N = 10000$. In (a)-(f) $K_3 = 0$ and QF coefficient (7) is employed, and in (g)-(h) $K_3 = 10^{-39} \text{ m}^6/\text{s}$, and zero QF coefficient is used. The shapes are always filament-like but can be short for a small number of atoms, viz. Figs. 7(a)-(c), long for a large number of atoms, viz. Figs. 7(e)-(f), fat in the self-repulsive case, viz. Figs. 7(d)-(f), and becomes thin as the self repulsion is reduced gradually, viz. Fig. 7(a), until self-attractive regime is attained, viz. Figs. 7(g)-(h). In general, the self-repulsive self-bound droplets are elongated along the z

direction and this length increases without bound with an increase of number of atoms N . This can be seen from Figs. 7(d)-(f) for $a = 90a_0$ as N increases from 10000 to 20000 and then to 40000, while other parameters are held fixed. Similarly, in the self-attractive case the length also increases with N , with other parameters held fixed (not illustrated here).

4. Summary

We studied the formation of trapless self-bound self-repulsive ($a > 0$) and self-attractive ($a < 0$) dipolar droplets in 3D in a strongly dipolar BEC of ^{164}Dy atoms of dipolar length $a_{\text{dd}} = 130.8a_0$. We used a beyond-mean-field model including the QF LHY interaction and a three-body interaction in addition to the usual two-body atomic contact and dipolar interactions of the mean-field GP equation. The usual two-body contact and dipolar interactions lead to a cubic nonlinearity in the mean-field GP equation. In 3D, the attractive cubic nonlinearity in the mean-field model leads to collapse and one cannot have a self-bound state [5]. But due to the beyond-mean-field QF LHY and/or three-body interactions with higher-order quartic and quintic nonlinearities, respectively, the collapse could be avoided and a strongly-dipolar BEC droplet can be formed. For $30a_0 \lesssim a < a_{\text{dd}}$, the imaginary part of the QF LHY interaction is small and both the LHY and/or three-body interactions can be used, as appropriate. But for $a \lesssim 30a_0$, the imaginary part of the LHY interaction becomes large and its use is not recommended [27]; in this region only the three-body interaction is used.

We consider a numerical solution and an analytic variational approximation of the beyond-mean-field model. The variational approximation with Gaussian ansatz for the wave function provides an analytic understanding of the formation of a strongly dipolar self-bound droplet. Such a droplet can be formed for number of atoms N larger than a critical value N_{cr} : $N > N_{\text{cr}}$. This critical number N_{cr} is a monotonically increasing function of the atomic scattering length a (K_3) for a fixed three-body coefficient K_3 (a). The increase of a and K_3 enhances the repulsive interaction in the system resulting in larger sizes of the self-bound droplet and also an increase in its negative energy. For a fixed N and K_3 , the negative energy of the system increases with a ; for $N = N_{\text{cr}}$ this energy becomes zero. For $N < N_{\text{cr}}$, the energy is positive and it is not possible to form a self-bound droplet. We presented numerical results for the integrated reduced densities (20) and (21) as well as the 3D isodensity contours of the self-bound dipolar droplets in good agreement with the analytic variational results. The 3D isodensity contours reveal that the shape of the droplet is always filament-like but can be long for a large number of atoms, short for a small number of atoms, fat for self-repulsive droplets or thin for self-attractive droplets. In view of the recent observation of trapped dipolar droplets in BECs of ^{164}Dy [18] and ^{168}Er [19] atoms, and of free-space binary self-bound droplets [13], the experimental observation of the present untrapped dipolar droplets in free space seems possible, with present knowhow, after a slow removal of the traps of a trapped dipolar droplet as was emphasized in Ref. [22].

Credit author statement

Both authors were responsible for Conceptualization, Methodology, and Software. L. E. Young-S. was responsible for Formal Analysis, Investigation, Data Curation and Writing - Original Draft. S. K. Adhikari was responsible for Writing - Review and Editing and Supervision.

Acknowledgments

S.K.A. acknowledges support by the CNPq (Brazil) grant 301324/2019-0, and by the ICTP-SAIFR-FAPESP (Brazil) grant 2016/01343-7.

References

- [1] Y. S. Kivshar, B. A. Malomed, *Rev. Mod. Phys.* 61, 763 (1989);
V. S. Bagnato, D. J. Frantzeskakis, P. G. Kevrekidis, B. A. Malomed, D. Mihalache, *Rom. Rep. Phys.* 67, 5 (2015); D. Mihalache, *Rom. J. Phys.* 59, 295 (2014).
- [2] Y. S. Kivshar, G. Agrawal, *Optical Solitons: From Fibers to Photonic Crystals*, (Academic Press, San Diego, 2003).

- [3] K. E. Strecker, G. B. Partridge, A. G. Truscott, R. G. Hulet, *Nature (London)* 417, 150 (2002);
L. Khaykovich, F. Schreck, G. Ferrari, T. Bourdel, J. Cubizolles, L. D. Carr, Y. Castin, C. Salomon, *Science* 256, 1290 (2002);
S. L. Cornish, S. T. Thompson, C. E. Wieman, *Phys. Rev. Lett.* 96, 170401 (2006).
- [4] V. M. Pérez-García, H. Michinel, H. Herrero, *Phys. Rev. A* 57, 3837 (1998).
- [5] R.Y. Chiao, E. Garmire, C.H. Townes, *Phys. Rev. Lett.* 13, 479 (1964).
- [6] S. K. Adhikari, *Phys. Rev. A* 103, L011301 (2021);
H. Sakaguchi, B. Li, B. A. Malomed, *Phys. Rev. E* 89, 032920 (2014);
S. Gautam, S. K. Adhikari, *Phys. Rev. A* 95, 013608 (2017);
Y.-C. Zhang, Z.-W. Zhou, B. A. Malomed, H. Pu, *Phys. Rev. Lett.* 115, 253902 (2015);
S. Gautam, S. K. Adhikari, *Phys. Rev. A* 97, 013629 (2018).
- [7] H. Sakaguchi, B. A. Malomed, *Phys. Rev. E* 90, 062922 (2014).
- [8] T. D. Lee, K. Huang, C. N. Yang, *Phys. Rev.* 106, 1135 (1957).
- [9] H.-W. Hammer, A. Nogga, A. Schwenk, *Rev. Mod. Phys.* 85, 197 (2013).
- [10] A. Bulgac, *Phys. Rev. Lett.* 89, 050402 (2002);
D. S. Petrov, *Phys. Rev. Lett.* 112, 103201 (2014).
- [11] D. S. Petrov, *Phys. Rev. Lett.* 115, 155302 (2015).
- [12] S. K. Adhikari, *Laser Phys. Lett.* 15, 095501 (2018).
- [13] C. R. Cabrera, L. Tanzi, J. Sanz, B. Naylor, P. Thomas, P. Cheiney, L. Tarruell, *Science* 359, 301 (2018);
G. Semeghini, G. Ferioli, L. Masi, C. Mazzinghi, L. Wolswijk, F. Minardi, M. Modugno, G. Modugno, M. Inguscio, M. Fattori, *Phys. Rev. Lett.* 120, 235301 (2018).
- [14] S. Will, T. Best, U. Schneider, L. Hackermüller, D. S. Lühmann, I. Bloch, *Nature (London)* 465, 197 (2010);
A. J. Daley, J. Simon, *Phys. Rev. A* 89, 053619 (2014).
- [15] F. Kh. Abdullaev, A. Gammal, Lauro Tomio, T. Frederico, *Phys. Rev. A* 63, 043604 (2001);
H. Al-Jibbouri, I. Vidanović, Antun Balaž, A. Pelster, *J. Phys. B* 46, 065303 (2013);
H.-C. Li, K.-J. Chen, J.-K. Xue, *Chin. Phys. Lett.* 27, 030304 (2010);
P. Ping, L. Guan-Qiang, *Chin. Phys. B* 18, 3221 (2009);
M. S. Mashayekhi, J.-S. Bernier, D. Borzov, J.-L. Song, F. Zhou, *Phys. Rev. Lett.* 110, 145301 (2013);
S. Mostafa Moniri, H. Yavari, E. Darsheshdar; arXiv:2109.08366.
- [16] A. J. Daley, J. M. Taylor, S. Diehl, M. Baranov, P. Zoller, *Phys. Rev. Lett.* 102, 040402 (2009);
L. Mazza, M. Rizzi, M. Lewenstein, J. I. Cirac, *Phys. Rev. A* 82, 043629 (2010);
M. Singh, A. Dhar, T. Mishra, R. V. Pai, B. P. Das, *Phys. Rev. A* 85, 051604(R) (2012).
- [17] M. Schmitt, M. Wenzel, F. Böttcher, I. Ferrier-Barbut, T. Pfau, *Nature (London)* 539, 259 (2016).
- [18] I. Ferrier-Barbut, H. Kadau, M. Schmitt, M. Wenzel, T. Pfau, *Phys. Rev. Lett.* 116, 215301 (2016).
- [19] L. Chomaz, S. Baier, D. Petter, M. J. Mark, F. Wächtler, L. Santos, F. Ferlaino, *Phys. Rev. X* 6, 041039 (2016).
- [20] A. R. P. Lima, A. Pelster, *Phys. Rev. A* 84, 041604(R) (2011);
A. R. P. Lima, A. Pelster, *Phys. Rev. A* 86, 063609 (2012).
- [21] F. Wächtler, L. Santos, *Phys. Rev. A* 93, 061603(R) (2016).
- [22] D. Baillie, R. M. Wilson, R. N. Bisset, P. B. Blakie, *Phys. Rev. A* 94, 021602(R) (2016).
- [23] D. Baillie, R. M. Wilson, P. B. Blakie, *Phys. Rev. Lett.* 119, 255302 (2017);
S. Pal, D. Baillie, P. B. Blakie, *Phys. Rev. A* 105, 023308 (2022).
- [24] F. Wächtler, L. Santos, *Phys. Rev. A* 94, 043618 (2016).
- [25] Z.-K. Lu, Y. Li, D. S. Petrov, G. V. Shlyapnikov, *Phys. Rev. Lett.* 115, 075303 (2015).
- [26] T. Ramakrishnan, S. Subramaniyan, *Phys. Lett. A* 383, 2033 (2019).
- [27] L. Chomaz, I. Ferrier-Barbut, F. Ferlaino, B. Laburthe-Tolra, B. L. Lev, T. Pfau, arXiv:2201.02672.
- [28] T. Lahaye, C. Menotti, L. Santos, M. Lewenstein, T. Pfau, *Rep. Prog. Phys.* 72, 126401 (2009).
- [29] R. Kishor Kumar, L. E. Young-S., D. Vudragović, A. Balaž, P. Muruganandam, S. K. Adhikari, *Comput. Phys. Commun.* 195, 117 (2015).
- [30] V. I. Yukalov, *Laser Phys.* 28, 053001 (2018).
- [31] Y. Tang, A. Sykes, N. Q. Burdick, J. L. Bohn, B. L. Lev, *Phys. Rev. A* 92, 022703 (2015).
- [32] M. Abad, M. Guilleumas, R. Mayol, M. Pi, D. M. Jezek, *Phys. Rev. A* 79, 063622 (2009);
M. Abad, M. Guilleumas, R. Mayol, M. Pi, D. M. Jezek, *Phys. Rev. A* 81, 043619 (2010).
- [33] R. N. Bisset, R. M. Wilson, D. Baillie, P. B. Blakie, *Phys. Rev. A* 94, 033619 (2016).
- [34] J. Söding, D. Guéry-Odelin, P. Desbiolles, F. Chevy, H. Inamori, J. Dalibard, *Applied Phys. B* 69, 257 (1999);
D. M. Stamper-Kurn, M. R. Andrews, A. P. Chikkatur, S. Inouye, H.-J. Miesner, J. Stenger, W. Ketterle, *Phys. Rev. Lett.* 80, 2027 (1998).
- [35] Y.-C. Zhang, F. Maucher, T. Pohl, *Phys. Rev. Lett.* 123, 015301 (2019);
Y.-C. Zhang, T. Pohl, F. Maucher, *Phys. Rev. A* 104, 013310 (2021).
- [36] J. Hertkorn, J.-N. Schmidt, M. Guo, F. Böttcher, K.S.H. Ng, S.D. Graham, P. Uerlings, T. Langen, M. Zwierlein, T. Pfau, *Phys. Rev. Research* 3, 033125 (2021);
F. Böttcher, J.-N. Schmidt, J. Hertkorn, K. S. H. Ng, S. D. Graham, M. Guo, T. Langen, T. Pfau, *Rep. Prog. Phys.* 84 012403 (2021).
- [37] P. Muruganandam, S. K. Adhikari, *Comput. Phys. Commun.* 180, 1888 (2009).
- [38] V. Lončar, L. E. Young-S., S. Škrbić, P. Muruganandam, S. K. Adhikari, A. Balaž, *Comput. Phys. Commun.* 209, 190 (2016).
- [39] S. Inouye, M.R. Andrews, J. Stenger, H.J. Miesner, D.M. Stamper-Kurn, W. Ketterle, *Nature (London)* 392, 151 (1998);
C. Chin, R.Grimm, P. Julienne, E. Tiesinga, *Rev. Mod. Phys.* 82, 1225 (2010).
- [40] F. K. Fatemi, K. M. Jones, P. D. Lett, *Phys. Rev. Lett.* 85, 4462 (2000).
- [41] A. Hammond, L. Lavoine, T. Bourdel, arXiv:2112.01782;
F. M. Gambetta, C. Zhang, M. Hennrich, I. Lesanovsky, W. Li, *Phys. Rev. Lett.* 125, 133602 (2020).